Stem Cell Research 22 (2017) 61–69

Contents lists available at ScienceDirect

Stem Cell Research

journal homepage: www.elsevier.com/locate/scr

Proteolytic processed form of CXCL12 abolishes migration and induces apoptosis in neural stem cells in vitro

Taís Adelita [a], Roberta Sessa Stilhano [b], Sang Won Han [b], Giselle Zenker Justo [a,c], Marimelia Porcionatto [a,*]

[a] Department of Biochemistry, Escola Paulista de Medicina, Universidade Federal de São Paulo, São Paulo, 04039, Brazil
[b] Department of Biophysics, Escola Paulista de Medicina, Universidade Federal de São Paulo, São Paulo, 04044, Brazil
[c] Department of Cell Biology, Universidade Federal de São Paulo, Diadema, 09920, Brazil

ARTICLE INFO

Article history:
Received 11 November 2016
Received in revised form 5 April 2017
Accepted 24 May 2017
Available online 4 June 2017

Keywords:
CXCL12
CXCL12(5-67)
Adult neural stem cell
Migration
Apoptosis
In vitro study

ABSTRACT

The subventricular zone (SVZ) of the adult mammalian brain hosts full potential neural stem cells (NSCs). NSCs are able to respond to extracellular signals in the brain, amplifying the pool of progenitor cells and giving rise to neuroblasts that show ability to migrate towards an injury site. These signals can come from vascular system, cerebrospinal fluid, glial cells, or projections of neurons in adjoining regions. CXCL12, a chemokine secreted after brain injury, reaches the SVZ in a gradient manner and drives neuroblasts towards the lesion area. Among many other molecules, matrix metalloproteinase 2 and 9 (MMP-2/9) are also released during brain injury. MMP-2/9 can cleave CXCL12 generating a new molecule, CXCL12(5-67), and its effects on NSCs viability is not well described. Here we produced recombinant CXCL12 and CXCL12(5-67) and evaluated their effect in murine adult NSCs migration and survival in vitro. We showed CXCL12(5-67) does not promote NSCs migration, but does induce cell death. The NSC death induced by CXCL12(5-67) involves caspases 9 and 3/7 activation, implying the intrinsic apoptotic pathway in this phenomenon. Our evidences in vitro make CXCL12(5-67) and its receptor potential candidates for brain injuries and neurodegeneration studies.

1. Introduction

Resident neural stem cells (NSCs) persist in the adult mammalian central nervous system (CNS) and encourage the search for potential treatments for neurodegenerative and acute brain diseases. Full potential stem cells (type B or astrocytes-like cells) line in the subventricular zone (SVZ) along the wall of the lateral ventricles in the brain. These cells are capable of proliferate, increasing the pool of progenitor cells through the generation of transient amplifying cells (type C cells) (Alvarez-Buylla and Garcia-Verdugo, 2002; Doetsch et al., 1997). The SVZ neurogenic niche comprises many components such as the vascular system, extracellular matrix, microglia, astrocytes, neurons, and cerebrospinal fluid (CSF), representing a countless source of stimuli to NSCs (Falcao et al., 2012; Lim and Alvarez-Buylla, 2014; Walton et al., 2006). The type C cells can give rise to oligodendrocytes or generate immature ("blasts") neurons called neuroblasts or type A cells in vivo (Doetsch et al., 1999). Together with type B and type C cells, neuroblasts are generally referred as neural progenitor cells (NPCs) and migrate along the rostral migratory stream (RMS) to the olfactory bulb (OB) (Lois and Alvarez-Buylla, 1994), where they differentiate into multiple types of interneurons (Lledo et al., 2008). During an injury, such as stroke (Arvidsson et al., 2002), traumatic brain injury (Ramaswamy et al., 2005), or neurodegenerative diseases (Saha et al., 2012), neuroblasts can migrate towards different areas of the CNS in response to signalling factors. Nevertheless, CNS regeneration process must overcome many obstacles besides NSCs expansion and migration, such as survival, differentiation into specific neural subtypes, and integration into a pre-existing neural network. Despite this capacity of neuroblasts to generate neurons in different CNS areas, the majority of them undergo apoptosis when arriving at a lesion site, resulting in absent or poor regeneration of adult mammalian brain (Arvidsson et al., 2002; Malone et al., 2012; Thored et al., 2006).

After a brain injury, soluble factors are released at the lesion site, reaching the SVZ through blood vessels, parenchymal diffusion or cell-cell communication. These factors provide cues that direct neuroblasts to the damaged areas. The chemokine CXCL12 (C-X-C motif ligand 12) – which also regulates homing and maintenance of stem cells in the niches – is among these factors (Kokovay et al., 2010). CXCL12, previously known as SDF-1 (stromal cell-derived factor 1), is a small secreted chemotactic cytokine composed of 67 amino acids. The N-terminus amino acid sequence of CXCL12 (KPVSLSYR, amino acids 1 to 8) (Fig. 1a) is critical for receptor activation and the sequence RFFESHI (amino acids 12 to 18) promotes the initial docking of the chemokine to its receptor CXCR4 (Crump et al., 1997). CXCL12 is abundant and selectively expressed in the developing and mature CNS (Tham et al., 2001), and is

* Corresponding author.
E-mail address: marimelia.porcionatto@unifesp.br (M. Porcionatto).

http://dx.doi.org/10.1016/j.scr.2017.05.013

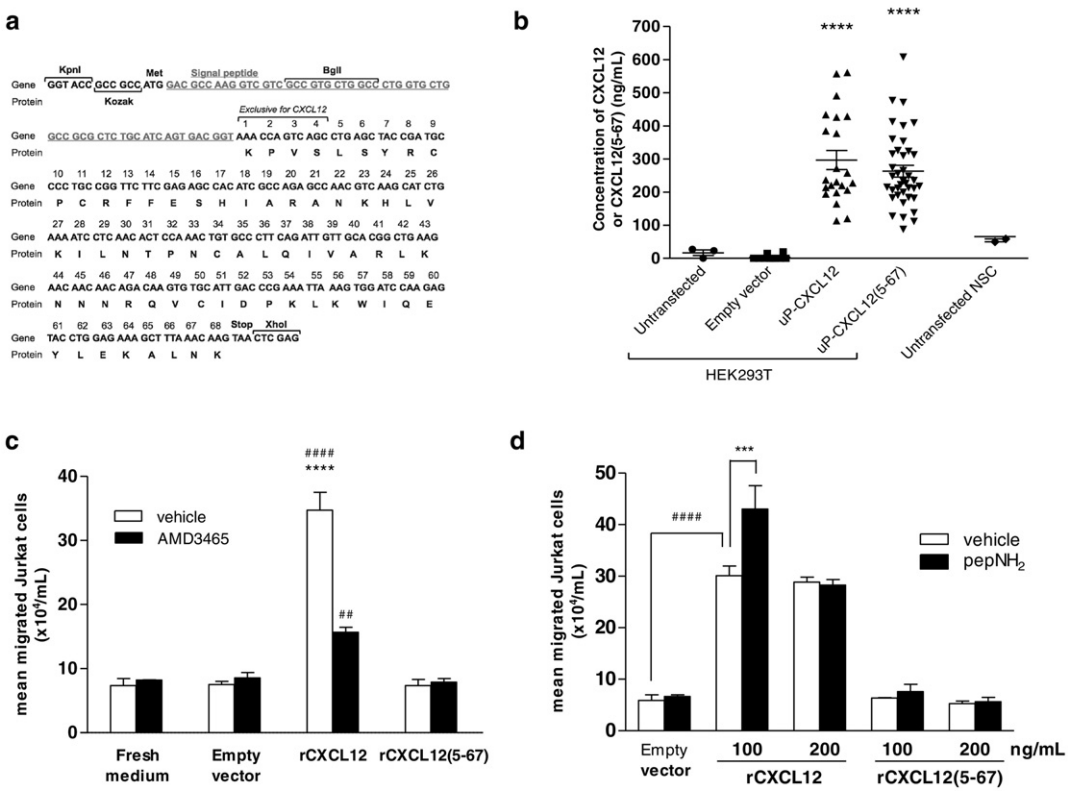

Fig. 1. Recombinant CXCL12 and CXCL12(5-67) production and their effect in Jurkat cells chemotaxis. (a) Nucleotides sequences inserted in the uP vector to produce rCXCL12 and rCXCL12(5-67). CXCL12 *Mus musculus* sequence was used as reference to synthesize the recombinant chemokines and KOZAC sequence was inserted before the signal peptide. *Kpn*I and *Xho*I restriction enzyme sites are flanking the coding sequence. *Bgl*I recognition site is identified and was used to check the insert presence in the vectors. CXCL12(5-67) lacks the first four amino acids from the full length chemokine (K, lysine; P, proline; V, valine; S, serine). (b) Level of rCXCL12 or rCXCL12(5-67) secreted by HEK293 and NSCs tested by ELISA. Untransfected: 1.9, SEM ± 23.2, $n = 3$; Empty vector: −49.3, SEM ± 12.9, $n = 10$; uP-CXCL12: 296.9, SEM ± 28.9, $^{****}P < 0.0001$ uP-CXCL12 vs. untransfected, $n = 22$; uP-CXCL12(5-67): SEM ± 17.8, $^{****}P < 0.0001$ uP-CXCL12 vs. untransfected, $n = 39$; Untransfected NSC: 54.3, SEM ± 4.3, $n = 2$. (c) Jurkat cells chemotaxis in the presence of 50 ng/mL of rCXCL12 or rCXCL12(5-67) and controls. The chemotactic activity was also determined in the presence of CXCR4 antagonist (AMD3465). Fresh medium: 7.3, SEM ± 1.1, and 8.2, SEM ± 0.04; Empty vector: 7.5, SEM ± 0.5, and 8.5, SEM ± 0.08; rCXCL12: 34.7, SEM ± 2.8, and 15.67, SEM ± 0.8, $^{****}P < 0.0001$ rCXCL12 vehicle vs. rCXCL12 AMD3465, $^{\#\#\#\#}P < 0.0001$ rCXCL12 vehicle vs. Fresh medium vehicle, and $^{\#\#}P = 0.0042$ rCXCL12 AMD3465 vs. Fresh medium AMD3465. Vehicle and AMD3465 values were presented in that order. $N = 3$. (d) Jurkat cells chemotaxis in the presence of 100 or 200 ng/mL of rCXCL12 or rCXCL12(5-67). The chemotactic activity was also determined in the presence of CXCL12 N-terminal peptide [KPVSLSYR-NH_2 (pep-NH2)]. Empty vector: 5.9, SEM ± 1.0, and 6.7, SEM ± 0.3; 100 ng/mL rCXCL12: 30.1, SEM ± 1.9, and 43.0, SEM ± 4.5, $^{***}P = 0.0003$ rCXCL12 vehicle vs. rCXCL12 pep-NH2, $^{\#\#\#\#}P < 0.0001$ rCXCL12 vehicle vs. Empty vector vehicle, and $^{\#\#\#\#}P < 0.0001$ rCXCL12 pep-NH2 vs. Empty vector pep-NH2; 200 ng/mL rCXCL12: 28.8, SEM ± 1.0, and 28.3, SEM ± 1.1, $^{\#\#\#\#}P < 0.0001$ rCXCL12 vehicle vs. Empty vector vehicle, and $^{\#\#\#\#}P < 0.0001$ rCXCL12 pep-NH2 vs. Empty vector pep-NH2. 100 ng/mL rCXCL12(5-67): 6.3, SEM ± 0.1, and 7.6, SEM ± 1.4; 200 ng/mL rCXCL12(5-67): 5.3, SEM ± 0.5, and 5.7, SEM ± 0.8. Vehicle and pep-NH2 values were presented in that order. $N = 3$. *Two-way or #one-way ANOVA.

secreted by endothelial cells, astrocytes, microglia and neurons (Banisadr et al., 2003). CXCR4 (C-X-C motif receptor 4) is the signalling G protein-coupled receptor of CXCL12, also widely expressed in the CNS (Banisadr et al., 2002).

The CXCL12/CXCR4 axis is involved in mobilization, proliferation, migration and differentiation of progenitor cells mainly during development but also in adulthood (Bajetto et al., 1999; Imitola et al., 2004; Itoh et al., 2009; McGrath et al., 1999; Tiveron et al., 2006). Constitutive expression of CXCL12 in the adult CNS is kept at a low level, and is upregulated under injury states, when then CXCL12 enhances the recruitment of neuroblasts from the SVZ neurogenic niche to lesion sites and provides signalling for a potential endogenous stem cell-based repair (for a review see Li et al., 2012).

Partial cleavage of CXCL12 at the N-terminus by distinct peptidases results in loss of chemotactic activity and impairment in CXCR4 receptor affinity (Cho et al., 2010; Delgado et al., 2001; Levesque et al., 2003). The proteolytic cleavage of CXCL12 by matrix metalloproteinase 2 and 9 (MMP-2 and 9) removes selectively the first four N-terminus amino acids from the full length molecule, generating the truncated form CXCL12(5-67) (McQuibban et al., 2001). Previous work (Denoyer et al., 2012; Van Raemdonck et al., 2014; Vergote et al., 2006; Zhu et al., 2009) showed that CXCR3, natural receptor of CXCL9, 10 and 11, acts as signalling receptor for CXCL12(5-67). These authors also demonstrated in those independent studies that CXCL12(5-67) affects the viability of differentiated cell types in the CNS, but its effect on neural stem cells remains poorly studied.

The aim of the present work was to investigate the activity of the truncated form of CXCL12, CXCL12(5-67), in NSCs viability. Herein we produced CXCL12 and CXCL12(5-67) recombinant and assessed their activity on adult murine NSCs migration and viability in vitro. Our data show, for the first time, that CXCL12(5-67) induces apoptosis in adult NSCs in vitro. The demonstration of an emerging role for CXCL12(5-67) in the low regenerative capacity of the CNS provides a basis for considering this cleaved form of CXCL12 as a novel target for treatment during traumatic brain and neurodegenerative diseases.

2. Results

2.1. CXCL12(5-67) is not chemotactic to CXCR4$^+$ cells

We constructed uP vectors containing either the native or the cleaved form of CXCL12 sequence and transfected HEK293T cells in order to produce CXCL12 and CXCL12(5-67) (Fig. 1a). Both forms of recombinant CXCL12 [rCXCL12 and rCXCL12(5-67)] were secreted in HEK293T conditioned medium. The concentration obtained was on average 296.9 ng/mL for rCXCL12 and 263.1 ng/mL for rCXCL12(5-67) (Fig. 1b). HEK293T cells transfected with empty uP vector and untransfected did not secret detectable amounts of CXCL12.

Additionally, adult NSCs cultivated as neurospheres secreted detectable amount of CXCL12 in the medium (mean 49.96 ng/mL).

To test the chemotactic activity of the recombinant proteins CXCL12 and CXCL12(5-67), we used Jurkat cells, a human T lymphocyte cell line that express high-affinity CXCR4 receptor and respond to chemotaxis promoted by CXCL12 (Hesselgesser et al., 1998). Conditioned medium from HEK293T cells transfected with empty vector did not induce chemotaxis, corroborating the result that showed HEK293T conditioned medium does not contain significant amounts of CXCL12 (Fig. 1c). As expected, rCXCL12 induced Jurkat cells chemotaxis and the specific CXCR4 antagonist (AMD3465) blocked this effect.

We have previously shown that a synthetic octapeptide analogous to CXCL12 N-terminus [KPVSLSYR-NH_2], here denominated pepNH_2, was not able to induce chemotaxis in NSCs (Filippo et al., 2013). Since pepNH_2 contains missing amino acids of CXCL12(5-67), here we asked whether pepNH_2 would be able to rescue the chemotactic activity when added together CXCL12(5-67). When pepNH_2 – which contains CXCR4 receptor activation domain – was added to the Jurkat cells together with rCXCL12(5-67) (which preserves CXCR4-docking domain), no chemotaxis was observed. More, CXCL12(5-67) did not induce chemotaxis even when higher concentrations were tested (Fig. 1d). Unexpectedly, pepNH_2 increased chemotaxis induced by 100 ng/mL, but not 200 ng/mL, of rCXCL12.

After confirmation that rCXCL12 secreted by transfected HEK293T cells preserves the chemotactic activity on CXCR4$^+$ cells, we evaluated the effect of the recombinant molecules, either rCXCL12 or rCXCL12(5-67), on NSCs migration (Fig. 2). Adult NSC were cultured as multicellular free-floating spheres (neurospheres) and, after adhesion to a laminin-coated surface, were treated with the recombinant chemokines. We considered the distance that cells reached outside the sphere contour as a measure of migration. As expected, rCXCL12(5-67) did not induce NSC migration when compared to cells treated with empty vector (Fig. 2a, b). On the other hand, rCXCL12 was able to increase in 30% the distance NSCs migrated when compared to fresh medium or conditioned medium from cells transfected with empty vector.

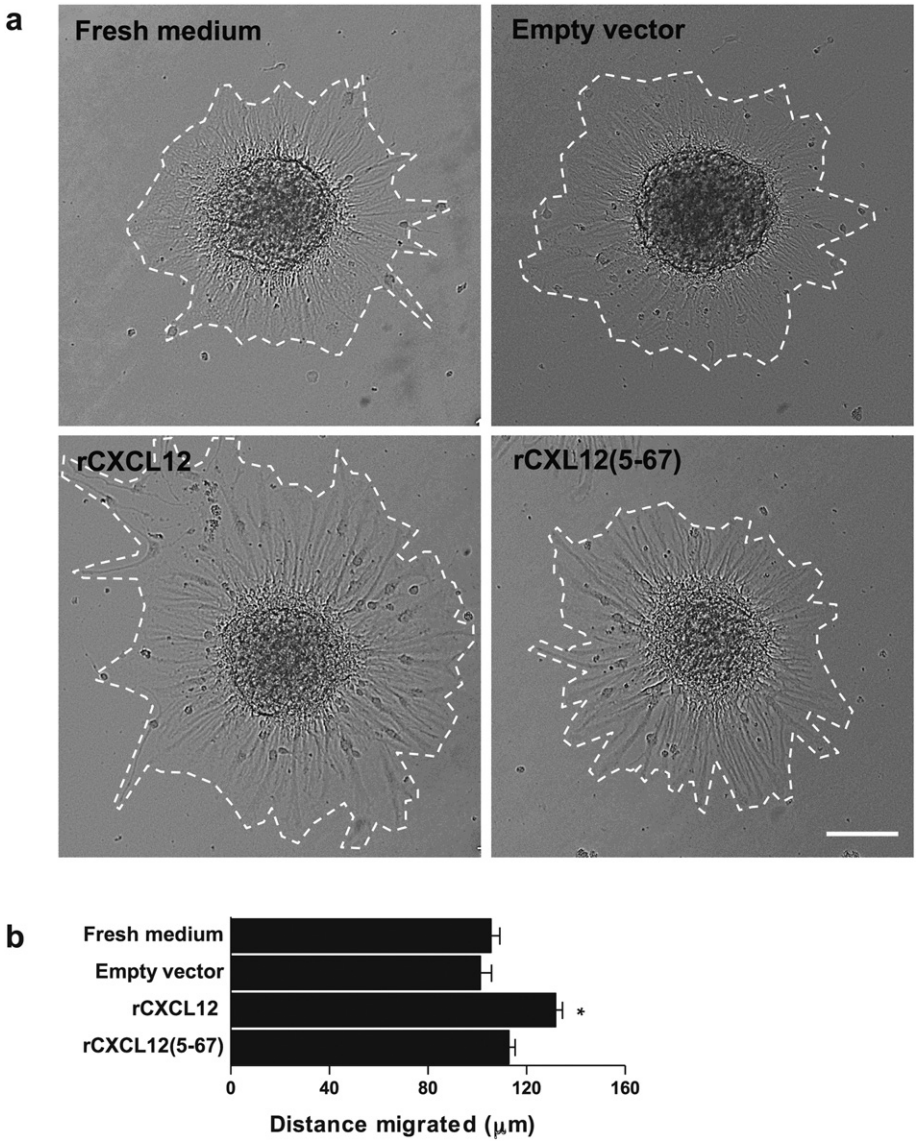

Fig. 2. Effects of CXCL12 and CXCL12(5-67) on neural stem cell migration in vitro. (a–b) Neurospheres were treated for 24 h with 50 ng/mL rCXCL12, rCXCL12(5-67) or controls and had the radii measured in three different areas, starting from the edge of the sphere to the farthest migrated cell. The average of these values for each sphere is plotted in the graph. Fresh medium: 103.5, SEM ± 4.3, $n = 28$; Empty vector: 99.4, SEM ± 4.8, $n = 26$; rCXCL12: 130.8, SEM ± 4.4, $n = 31$, $^{***}P < 0.0001$ rCXCL12 vs. Empty vector; rCXCL12(5-67): 114.8, SEM ± 3.6, $n = 34$. Bar: 100 μm.

2.2. CXCL12(5-67) induces neural stem cell death

Despite NSCs have been described as less susceptible to cytotoxicity than differentiated cells (Brazel et al., 2014), we hypothesised CXCL12(5-67) could be inducing apoptosis in NSCs, implicating this molecule in the poor spontaneous regeneration of the CNS. As an indicator of early apoptosis, we evaluated the translocation of phosphatidylserine (PS) to the outer leaflet of the plasma membrane using annexin V-binding assay. Neurospheres were dissociated and NSCs were cultured for 24 h on laminin-coated coverslips. We evaluated PS translocation after 24 h of treatment with rCXCL12(5-67), rCXCL12, or staurosporine as positive control (a pleiotropic kinase inhibition that induces cell death). rCXCL12(5-67) induced PS translocation in NSCs in comparison with empty vector or rCXCL12 treatments (Fig. 3a,b), suggesting that rCXCL12(5-67) induces apoptosis in NSCs.

2.3. CXCL12(5-67) activates intrinsic pathway of apoptosis in NSCs

Annexin V assay suggested CXCL12(5-67) induces apoptosis in NSCs, but because even a transient loss of the plasma membrane integrity allows annexin V binding regardless of whether or how the cells die, we decided to confirm the effect of rCXCL12(5-67) in NSCs by assessing cleavage of caspases 3 and 7, since their activation is involved in apoptotic cell death pathways.

The treatment of NSCs with rCXCL12(5-67) for 4, 6 or 24 h induced activation of caspases 3/7 when compared to control (fresh medium) or rCXCL12 (Fig. 4 a) confirming the apoptosis-mediated cell death induced by CXCL12(5-67). In order to investigate which apoptotic pathway is involved in the CXCL12(5-67)-induced cell death, we measured the activation of caspase 8 (extrinsic pathway) and caspase 9 (intrinsic pathway) in NSCs treated with rCXCL12(5-67) in vitro. Caspase 9 (Fig. 4c) was activated by rCXCL12(5-67), but caspase 8 did not (Fig. 4b),

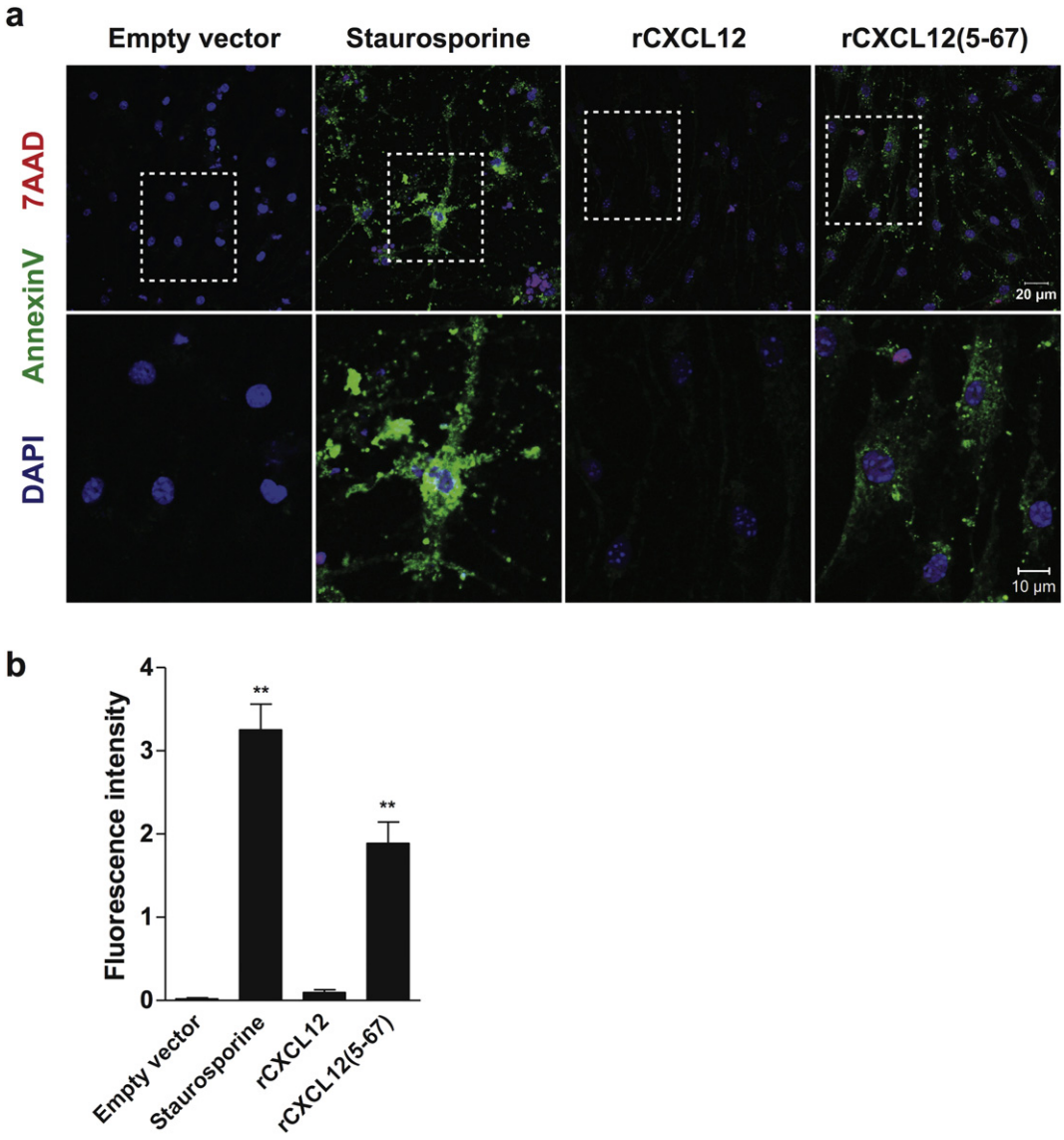

Fig. 3. Apoptosis detection by annexin V binding assay in NSC treated with CXCL12 and CXCL12(5-67). (a–b) NSC isolated from neurospheres and cultured for 24 h with 1 μM staurosporine, 200 ng/mL rCXCL12 or CXCL12(5-67). Exteriorised phosphatidylserine (PS) is demonstrated by annexin V binding (green). Empty vector: 0.02, SEM ± 0.01; Staurosporine: 3.26, SEM ± 0.3, $^{**}P = 0.0017$ Staurosporine vs. Empty vector; rCXCL12: 0.09, SEM ± 0.03; rCXCL12(5-67): 1.9, SEM ± 0.3, $^{**}P = 0.0037$ rCXCL12(5-67) vs. Empty vector. $N = 4$ areas in the picture. 7AAD (red), and DAPI (blue). Bars: 20 μm (upper set) and 100 μm (bottom set).

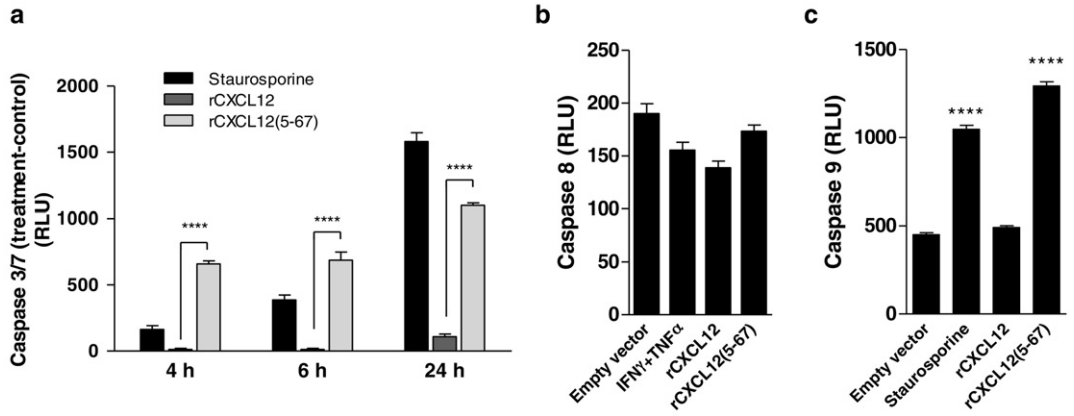

Fig. 4. Activation of caspases in NSCs treated with CXCL12 and CXCL12(5-67). (a) Caspases 3 and 7 activation evaluation in dissociated NSCs treated with empty vector media (value subtracted from all treatments), 1 μM staurosporine, 200 ng/mL rCXCL12 or 200 ng/mL CXCL12(5-67) for 4, 6 or 24 h in independent experiments. Staurosporine: 164.1, SEM ± 28.4; 386.7, SEM ± 36.6; 1580, SEM ± 67.4. rCXCL12: −79.42, SEM ± 82.9; −201.9, SEM ± 19.75; 109.2, SEM ± 20.6. rCXCL12(5-67): 658.9, SEM ± 24.0; 686.7, SEM ± 62.9; 1099, SEM ± 18.9. Values presented in the following order: 4, 6 and 24 h. At 4 h: $^{****}P < 0.0001$ rCXCL12 vs. rCXCL12(5-67); At 6 h: $^{****}P < 0.0001$ rCXCL12 vs. rCXCL12(5-67); At 24 h: $^{****}P < 0.0001$ rCXCL12 vs. rCXCL12(5-67). 4 and 6 h, $n = 10$; 24 h, $n = 11$. (b) Caspase 8 activation evaluation in dissociated NSCs treated with empty vector media, 1 ng/mL IFN-γ + 4 ng/mL TNF-α, 200 ng/mL rCXCL12 or CXCL12(5-67). Empty vector: 190.1, SEM ± 9.4; IFN + TNF: 155.5, SEM ± 7.4; rCXCL12: 139, SEM ± 6.2; rCXCL12(5-67): 173.5, SEM ± 5.8. $N = 11$. (c) Caspase 9 activation evaluation in dissociated NSCs treated with empty vector media, 1 μM staurosporine, 200 ng/mL rCXCL12 or CXCL12(5-67). Empty vector: 450.9, SEM ± 10.7; Staurosporine: 1047, SEM ± 22.2; rCXCL12: 492.1, SEM ± 9.8; rCXCL12(5-67): 1293, SEM ± 23.3. $N = 11$. $^{****}P < 0.0001$ Staurosporine vs. Empty vector; $^{****}P < 0.0001$ rCXCL12(5-67) vs. Empty vector. RLU: relative luminescence units.

confirming CXCL12(5-67) induced cell death through the intrinsic pathway of apoptosis.

2.4. NSCs express CXCR3 receptor and CXCL9 ligand prevents CXCL12(5-67)-induced caspases activation

CXCL12(5-67) has been described to lose its original affinity for CXCR4 receptor and to bind to CXCR3 receptor (Denoyer et al., 2012; Vergote et al., 2006; Zhu et al., 2009). In order to confirm that CXCL12(5-67) induces cell death by targeting other receptor than CXCR4, we repeated caspases 3/7 activation experiment but at this time adding the selective CXCR4 antagonist, AMD3465. As expected, rCXCL12(5-67) with CXCR4 antagonist continued inducing caspases 3/7 activation, confirming CXCR4 receptor does not mediate CXCL12(5-67) activity (Fig. 5 a).

Since CXCR3 has been implicated as a receptor targeted by CXCL12(5-67), we assessed CXCR3 expression in NSCs and astrocytes in vitro by PCR. Astrocytes as well as NSCs cultivated from naive mice or animals submitted to traumatic brain injury (TBI) showed to express CXCR3 receptor (Fig. 5b). In order to corroborate the findings from other groups showing CXCL12(5-67) binds to CXCR3 we took advantage from the affinity between CXCR3 and its natural ligand CXCL9 (Cole et al., 1998) to assess CXCL12(5-67)-CXCR3 affinity. We incubated NSCs with CXCL9 for 1 h at 4 °C to allow receptor-ligand binding and to avoid or delay receptor internalization and recycling as well as cell signalling. After this period, cells were treated with rCXCL12, rCXCL12(5-

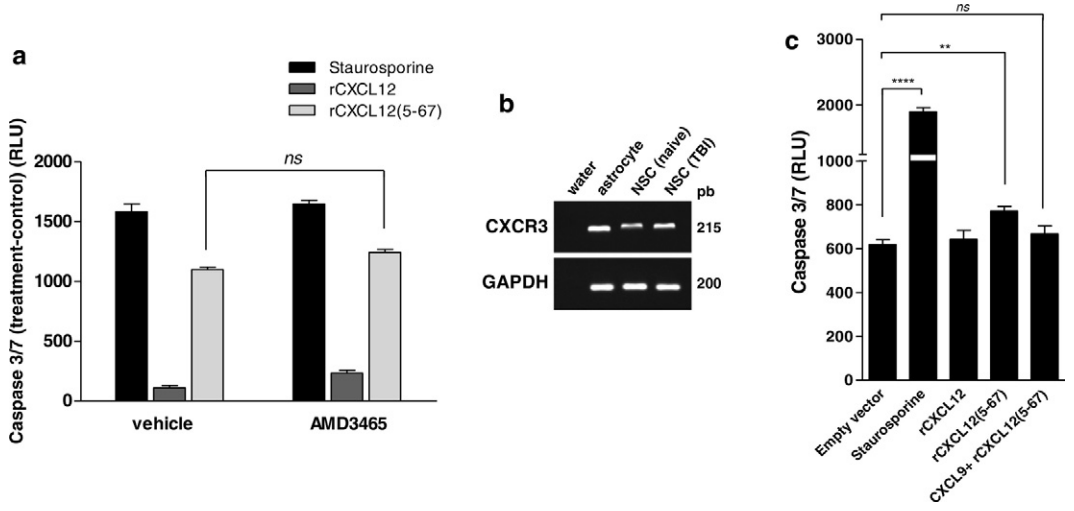

Fig. 5. CXCL12(5-67) induces caspases activation through CXCR3 and not CXCR4 receptor. (a) Caspases 3 and 7 activation evaluation in dissociated NSCs treated with empty vector media (value subtracted from all treatments), 1 μM staurosporine, 200 ng/mL rCXCL12 or CXCL12(5-67) for 24 h and in the presence of CXCR4 antagonist (AMD3465) or its vehicle pre-treatments for 1 h. Staurosporine plus vehicle: 1580, SEM ± 67.4; rCXCL12 plus vehicle: 109.2, SEM ± 20.6; rCXCL12(5-67) plus vehicle: 1099, SEM ± 18.9; Staurosporine plus AMD3465: 1646, SEM ± 31.9; rCXCL12 plus AMD3465: 232.6, SEM ± 24.9; rCXCL12(5-67) plus AMD3465: 1240, SEM ± 25.6. $N = 11$. (b) Conventional PCR showing expression of CXCR3 receptor in NSCs cultured from naive or traumatic brain injured (TBI) mice and astrocytes. GAPDH was used as housekeeping gene. Full-length gel is presented in Supplementary Fig. 2. (c) NSCs pre-treated with vehicle or 200 ng/mL CXCL9 (last bar) for 1 h at 4 °C. After that, NSCs received empty vector supernatant, 1 μM staurosporine, 200 ng/mL rCXCL12 or CXCL12(5-67) for 4 h and then were assessed for caspase 3/7 activation. Empty vector: 617.5, SEM ± 22.8; Staurosporine: 1896, SEM ± 62.4; rCXCL12: 641.8, SEM ± 41.8; rCXCL12(5-67): 771.6, SEM ± 21.5; CXCL9 + rCXCL12(5-67): 667, SEM ± 36.7. $N = 10$. $^{****}P < 0.0001$ Staurosporine vs. Empty vector; $^{**}P = 0.006$ rCXCL12(5-67) vs. Empty vector; $P = 0.0815$ rCXCL12(5-67) vs. CXCL9 + rCXCL12(5-67). RLU: relative luminescence units.

67) or controls (empty vector or Staurosporine) and left to recover at 37 °C for 4 h. As we anticipated, CXCL9 pre-treatment prevented rCXCL12(5-67) caspases 3/7 activation (Fig. 5c), suggesting that CXCL9 and rCXCL12(5-67) bind to the same receptor, CXCR3.

3. Discussion

In the healthy brain, MMP-2/9 modulate neural progenitor cell migration from the SVZ to the olfactory bulb along the rostral migratory stream (Bovetti et al., 2007), whereas following brain lesions, MMP-2/9 participate on migration of neural progenitors into an injured area. Besides migration, MMPs play regulatory activity in different tissues, processing active molecules as surface receptors, growth factors and chemokines (Ben-Hur et al., 2006; Kang et al., 2008; Lee et al., 2006). CXCL12 is one of the many substrates of MMP-2/9, and cleavage in a specific site at N-terminal portion of CXCL12 generates CXCL12(5-67) (McQuibban et al., 2001). In addition, enhanced MMP-2/9 expression is involved in the pathophysiologic mechanisms of brain injury and neurodegenerative diseases (Hoehna et al., 2012; Kaplan et al., 2014; Stomrud et al., 2010; Uckermann et al., 2011).

Here we showed that CXCL12(5-67) impairs NSCs migration. These results corroborated with the reports of Peng et al. (2012) which demonstrated that the proteolytic processing of CXCL12 by MMP-2/9 reduces foetal neural progenitor cell migration. We also observed no difference on migration when we increased CXCL12(5-67) concentration, suggesting a migration abolishment rather than receptor affinity reduction. These findings are in accordance with many other studies showing that most of CXCL12 receptor activation sequence disrupts migration mediated by CXCR4 receptor. When we tried to recover the full-length molecule chemotactic capacity by adding CXCL12 N-terminal peptide (KPVSLSYR-NH_2, pep NH_2) together with CXCL12(5-67), still no effect on migration was observed. This observation indicates that the spatial arrangement of these sequences in the full-length molecule is important for binding and activation of CXCR4 receptor.

Chemokines have been reported to act in an optimal concentration, with no improvement in the cell migration when concentration increases (Ottoson et al., 2001; Poznansky et al., 2000). Furthermore, it was reported that an increase in CXCL12 concentration above the optimal range blocks cell migration by ligand dimer formation, downregulation of receptor expression or its desensitization (Pelletier et al., 2000). Corroborating these observations, here we saw no difference in migration when cells were treated with increasing concentrations of CXCL12. Surprisingly, the N-terminal peptide enhanced CXCL12 chemotaxis at 100 ng/mL, but caused no effect at 200 ng/mL. Since the peptide per se does not induce chemotaxis, the effect observed may be due to an interaction between the peptide and the full-length molecule, preventing CXCL12 dimer formation, thus improving the chemotactic activity. Additionally, high concentrations of CXCL12 can induce dimerization of CXCR4 receptors, affecting signal transduction, which also can help to explain why CXCL12 chemotactic effect is not concentration dependent (Zlatopolskiy and Laurence, 2001).

As migration is one of multiple steps of neurogenesis, disruption of this process can ultimately affect newborn neurons survival. But here we aimed to assess the direct effect of CXCL12(5-67) on NSCs survival. Even though CXCL12(5-67) has been implicated in neurodegeneration by HIV and retinal degeneration (Denoyer et al., 2012; Vergote et al., 2006; Zhang et al., 2003), but its role in adult NSCs remained unclear. Here we showed, for the first time, that CXCL12(5-67) induces the intrinsic apoptosis pathway in adult NSCs. Treatment with CXCL12(5-67) induced activation of caspases 3 and 7 early as after 4 h of treatment in vitro, and apoptosis was also confirmed using the annexin V binding assay.

CXCL12(5-67) activity has been shown to occur through CXCR3 receptor, but its expression in neural stem cell remained a point of controversy. Here, we also showed that NSCs from traumatic brain injured and naive animals cultivated in vitro express CXCR3. Since astrocytes are in close contact to NSCs, we also decided assess whether that cell type could be a target for CXCL12(5-67) by expressing CXCR3 receptor. Once CXCL12(5-67) acted directly on NSCs, we did not investigate secondary effects of CXCL12(5-67) by CXCR3 activation of astrocytes. Based on these findings, a possible role for CXCL12(5-67)-CXCR3 axis on newborn cell death in the brain is proposed, making in vivo investigations necessary to confirm this hypothesis.

The activity of CXCL12(5-67) through CXCR3 receptor has been shown before (Denoyer et al., 2012; Zhu et al., 2009). Here we aimed to confirm this finding using CXCL9, a natural ligand of CXCR3. NSCs pre-treated with CXCL9 were not susceptible to the CXCL12(5-67) apoptotic effects. The effect of CXCL12(5-67) on NSCs in this set of experiments were less prominent then before, but still significant. This result can be explained by the fact that the cells were kept for 1 h at 4 °C, which keeps the viability but reduces the metabolic activity, enzymatic reactions rates, as well as transcription and translational processes (Hunt et al., 2005; Sonna et al., 2002).

4. Conclusions

The chemokine cleavage is a physiological process and represents an endogenous mechanism to inactivate soluble factors and then control their activity. The findings described here highlighted, for the first time, the involvement of the CXCL12 cleaved form, CXCL12(5-67), in neural stem cell death in vitro. These results provide basis for an in vivo investigation, where apoptosis of neuroblasts could be assessed in brain injuries and neurodegenerative diseases models. The CXCL12(5-67) occurrence is consistent with the environment generated after neuronal cell death, where neuroblasts are recruited from SVZ and follow the CXCL12 gradient, as well as MMP-2 and 9 are released during cell migration. Our data support the hypothesis that CXCL12(5-67) is responsible for NSC death during brain injury and diseases, and in vivo experiments should be conducted in order to confirm it. We suggest that following a cortical injury, CXCL12 is secreted at the injured area attracting neuroblasts from SVZ. Activated MMP-2/9 collaborates with neuroblasts migration through extracellular matrix remodelling, but also cleaves CXCL12. This process generates CXCL12(5-67) that activates the intrinsic apoptosis pathway via activation of CXCR3, leading to cell death.

5. Methods

5.1. Production of recombinant CXCL12 and CXCL12(5-67) by HEK293T cells

CXCL12 [GenBank: L12029] and CXCL12(5-67) DNA sequences preceded by Kozak sequence (GCCGCC) were synthesized by GenScript using pUC57 vector. The sequences of either forms of CXCL12 were digested with restriction enzymes *Kpn*I and *Xho*I, and cloned into the uP vector containing the cytomegalovirus (CMV) promoter and polycloning (Sacramento et al., 2010), generating uP-CXCL12 and uP-CXCL12(5-67) plasmids. Plasmids were amplified and purified using an endotoxin free plasmid kit (Qiagen). HEK293T cells were grown in DMEM supplemented with 10% heat-inactivated foetal calf serum (FCS) and used for transfection after trypsin-EDTA dissociation. Twenty-four hours before transfection, cells were seeded on a 60 mm dish at a density of 1×10^6 cells. One hour before transfection, the medium was replaced with a medium containing 0.5% FCS and cells were transfected using FuGENE (Promega) with 6 μg of DNA. Supernatant was collected after 48 h, centrifuged at $500 \times g$ for 10 min at RT, filtrated by 0,22 μm membrane pore and kept at −20 °C.

5.2. ELISA

Quantification of recombinant CXCL12 and recombinant CXCL12(5-67) secreted by HEK293T cells into the culture medium was performed

using mouse CXCL12/SDF-1 DuoSet DY460 (R&D) following the manufacturer's instructions. Briefly, the capture antibody was diluted in phosphate buffered saline (PBS) at a final concentration of 2 μg/mL and adsorbed overnight. Blockage was done with PBS containing 1% bovine serum albumin (BSA) for 2 h. A seven point standard curve using two-fold serial dilutions was done starting at 3 ng/mL and performed in triplicate, and the samples were quantified in duplicates for each dilution (1:125, 1:250, 1:500). Plates were incubated for 2 h. The detection antibody was used at a final concentration of 400 ng/mL with 2% normal goat serum (NGS). Streptavidin-horseradish peroxidase (HRP) was diluted at 1:200 and incubated for 20 min. The substrate solution used was 0.3% of *o*-phenylenediaminedihydrochloride (OPD) in citric acid solution, pH 5.0, for 20 min. The reaction was interrupted using 2 N H_2SO_4 and the optical density was determined using a microplate reader set at 490 nm VersaMax Absorbance Microplate Reader (Molecular Devices).

5.3. Chemotaxis assay

To analyze the capacity of recombinant CXCL12 and recombinant CXCL12(5-67) to attract $CXCR4^+$ cells, Jurkat cells were maintained at a density of 1×10^5 cells/mL in RPMI1640 medium with 10% FCS, 1% glutamine, and 1% penicillin/streptomycin antibiotics. To perform the chemotaxis assay, cells were centrifuged at $90 \times g$ for 3 min at RT, and suspended in free serum RPMI1640 medium at a density of 1×10^6 cells/mL. 700 μL of conditioned medium produced by HEK293T transfected cells with empty uP, uP-CXCL12 or uP-CXCL12(5-67) plasmids were added to the bottom of 24 well plates. After that, 200 μL of cell suspension were placed on the upper transwell chamber of 8 μm inserts (Millipore). The plate with the chambers was incubated for 4 h at 37 °C and 5% CO_2. Cells that migrated to the bottom of the well were recovered and counted in a haemocytometer. When CXCR4 antagonist was added, 8 μM of AMD3465 (Tocris) or vehicle were added to the cells for 40 min before place the cells in the inserts.

5.4. Animals

All animals were obtained from UNIFESP Animal Facility and all experiments were carried under protocols approved by the Research Ethics Committee (CEP) from Universidade Federal de São Paulo (CEP 1223/11).

5.5. Isolation of adult NSCs and neurospheres formation

Adult NSCs were obtained from the SVZ of 45 days old C57BL/6 female mice. After euthanasia by cervical dislocation, brain was removed, the SVZ dissected in the sagittal plain, and the tissue maintained in DMEM/F12. After sedimentation, supernatant was discarded, and cells were dissociated by incubation with 0.1% trypsin/EDTA during 5 min at 37 °C. To stop trypsin action, 10% FCS was added and cells were centrifuged for 5 min at $130 \times g$, and supernatant was removed. Isolated cells were then suspended in DMEM/F12 1:1 (v/v), supplemented with 2% B27, 20 ng/mL EGF, 20 ng/mL FGF2, 1% penicillin/streptomycin, and 5 μg/mL heparin. Cells were filtered in 40 μm nylon membrane and plated on a poly(2-hydroxyethyl metracrylate) (poly HEMA) pre-coated 75 cm^2 flask to avoid adhesion. Cells obtained from 4 mice were used in each flask. Neurospheres formation takes up to 5 days to occur, and during this time culture medium was partially changed after 2–3 days by centrifugation for 5 min at $100 \times g$. After the neurospheres reach a diameter around 100 μm, the spheres were mechanically dissociated, plated in 4 flasks also coated with poly HEMA and cultured until new neurospheres be formed. Secondary spheres were used to perform all experiments. For assays in which cells needed to be counted, the neurospheres were dissociated, filtered in 40 μm nylon membrane, and isolated cells were counted in a haemocytometer.

5.6. NSC migration assay

Neurospheres were plated in 24-well 10 μg/mL poly-L-lysine (Sigma-Aldrich) and 50 μg/mL laminin (UNIFESP) coated plates for 24 h to allow adhesion to the plate surface. Once neurospheres adhered, cells tended to leave the sphere, migrating outwards in a randomly fashion. The neurospheres were treated by an additional 24 h with rCXCL12 or rCXCL12(5-67) and, at the end of the incubation period, cells were photographed using an inverted microscope (Olympus). For NSC migration analysis, the distance from the edge of the sphere to the farthest migrated cells was measured at three distinct locations per sphere using ImageJ, and the average of this value was plotted in the graph.

5.7. Caspase activation assays

Caspases 3/7, 8 and 9 were measured using Caspase-Glo Assay kit (Promega) according to the manufacturer's instructions. Briefly, NSCs were seeded on a 96-well plate at a density of 1×10^4 cells and incubated for 24 h to allow neurospheres attachment. Cells were treated for different periods of time followed by 1 h incubation at 37 °C with Caspase-Glo. The luminescence produced is proportional to caspase activity and was quantified in the supernatant using FlexStation 3 Microplate Reader and SoftMax Pro (Molecular Devices). A negative control consisting of cells that were not treated was also included in each assay. As positive controls, 1 μM staurosporine or 1 ng/mL IFN-γ and 4 ng/mL TNF-α (R&D) were used to induce caspase activity. When CXCR4 antagonist was used, 8 μM of AMD3465 or vehicle were added to the cells for 1 h before chemokine treatments. For the CXCR3 competition experiment, cells were pre-treated for 1 h at 4 °C with 200 ng/mL of recombinant CXCL9 (Life Technologies) (as described by Uppaluri et al. (2008) with modifications), and then treated with rCXCL12, rCXCL12(5-67) or controls.

5.8. Annexin V and 7AAD staining and fluorescence image analysis

Apoptosis was measured using Annexin V binding followed by fluorescence microscopy analysis. Briefly, neurospheres were dissociated and isolated cells were cultured for 24 h on glass coverslips coated with poly-L-lysine and laminin. After that, cells were treated for 24 h with rCXCL12, rCXCL12(5-67) or staurosporine, the medium was removed and cells washed with PBS before staining. Annexin V-FITC (BD Pharmigen) and 7-amino-actinomycin D-PE (7AAD) for nuclear staining (Life Technologies) were both diluted in 1× binding buffer and cells were stained for 15 min at 37 °C in the dark, then washed twice with 1× binding buffer, fixed with 4% PFA and mounted with Prolong Gold Antifade with DAPI (Life Technologies). Immunofluorescence visualization was performed using a confocal microscope LSM 780-NLO (Zeiss). Fluorescence intensity was quantified using ImageJ by measuring four different and exclusive areas in the same figure. The error bar represents how the signal was homogenous (or not) in the field of view.

5.9. Primary cortical astrocytes culture

Astrocyte culture was prepared from cerebral hemispheres of 2 day-old C57BL/6 mice. Brain cortices from the newborn pups were aseptically removed and meninges were excised carefully. The tissue was mechanically dissociated and then filtered through a 40 μm nylon membrane. The filtered cells containing astrocytes were suspended in DMEM supplemented with 10% FCS, antibiotics and seeded in 75 cm^2 tissue culture flasks at a density of 1×10^7 cells. Cells were incubated at 37 °C in a humidified atmosphere containing 5% CO_2. After two days the flask was vigorously shook to detach microglia and all the supernatant was discarded. The medium was totally replaced and changed every two days. Astrocytes were subcultured when reached confluence and then plated to perform the experiments. Astrocytes were characterized with GFAP and S100B by immunocytochemistry.

5.10. Mice traumatic brain injury (TBI) model

Injury to mouse primary motor cortex (M1) was performed in 45 days old C57BL/6 mice as previously described Chiba et al., 2004; Coulson-Thomas et al., 2008). The animals were anesthetized using 100 μL of 2.5% 2,2,2-Tribromoethanol (Sigma Aldrich) intraperitoneally and positioned in the stereotaxic apparatus. A metal needle was chilled using isopentane on dry ice and was inserted 4 times, during 30 s each, into the motor cortex (stereotaxic coordinates from bregma: AP +0.198 mm; ML +0.175 mm; DV −0.15 mm). After surgery, the animals were kept warm and received acetaminophen at drink water. The SVZ was dissected 24 h after the injury and the neural stem cells grown according to isolation of adult NSC and neurospheres formation protocol.

5.11. RT-PCR

Total RNA from astrocytes or neurospheres obtained from TBI or naive animals was extracted using TRIzol protocol and quantified using GE NanoVue Spectrophotometer. Two micrograms of total RNA were reverse-transcribed with Oligo(dT)15 Primer and ImProm-II Reverse Transcription System (Promega) protocol. A negative control with all constituents but without DNA was included in the PCR reaction. The primers used were CXCR3: sense 5′ TACCTATCAGCCAACTACGATCA 3′, antisense: 5′ ACCACTACCACTAGCCTCATAG 3′; and GAPDH sense: 5′ TTCGACAGTCAGCCGCATCTTCTT 3′, and antisense: 5′ GCCCAATACGACCAAATCCGTTGA 3′.The thermal cycling conditions were 2 min at 92 °C, and 35 cycles of 30 s at 94 °C, 30 s at 60 °C, 30 s at 72 °C, and 5 min at 72 °C. The products were submitted to electrophoretic run in 1.8% agarose, 80 V, 1 h, stained with Blue Green loading dye (LGC) and revealed after ultraviolet incidence using BioRad ChemiDoc. The gene ruler low range DNA ladder (Fermentas) was applied in all runs.

5.12. Statistical analysis

Data were expressed as mean ± SEM from technical replicates (N), and the data were evaluated statistically by analysis of variance (ANOVA) followed by the Bonferroni test. The difference between values was considered statistically significant when the $P < 0.05$. The symbols meaning are as follow: $^{*}P < 0.05$, $^{**}P < 0.01$, $^{***}P < 0.001$, $^{****}P < 0.0001$. The GraphPad Prisma 5 was used for statistical analysis and graphing. To determine the *p*-value, QuickCalcs at <graphpad.com/quickcalcs/pValue2/> was used.

Author contributions

T.A. carried out and analyzed all experiments, co-developed the concept, and wrote the manuscript. R.S.S. co-performed the transfection experiments. S.W.H. contributed to the concept, shared reagents, and revised the manuscript. G.Z. shared reagents, contributed to the concept, analysis and interpretation of data, and revised the manuscript. M.P. developed the concept, coordinated the study, analysis and interpretation of data, and co-wrote the manuscript. All authors read and approved the final manuscript.

Competing interests

The authors declare that they have no competing interests.

Acknowledgements

We thank M.V. Palladino for technical assistance and F.G. Serrano for the artwork. We are grateful for the following financial support: FAPESP [2011/11388-4 (T.A.), 2012/00652-5 and 2015/19231-8 (M.P. – Research Grant)], and CNPq [404646/2012-3 (M.P. – Research Grant)]. Graphic abstract was designed by Felipe G. Serrano (www.illustrative-science.com).

Appendix A. Supplementary data

Supplementary data to this article can be found online at http://dx.doi.org/10.1016/j.scr.2017.05.013.

References

Alvarez-Buylla, A., Garcia-Verdugo, J.M., 2002. Neurogenesis in adult subventricular zone. J. Neurosci. 22, 629–634.
Arvidsson, A., Collin, T., Kirik, D., Kokaia, Z., Lindvall, O., 2002. Neuronal replacement from endogenous precursors in the adult brain after stroke. Nat. Med. 8, 963–970.
Bajetto, A., et al., 1999. Glial and neuronal cells express functional chemokine receptor CXCR4 and its natural ligand stromal cell-derived factor 1. J. Neurochem. 73, 2348–2357.
Banisadr, G., et al., 2002. Neuroanatomical distribution of CXCR4 in adult rat brain and its localization in cholinergic and dopaminergic neurons. Eur. J. Neurosci. 16, 1661–1671.
Banisadr, G., Skrzydelski, D., Kitabgi, P., Rostene, W., Parsadaniantz, S.M., 2003. Highly regionalized distribution of stromal cell-derived factor-1/CXCL12 in adult rat brain: constitutive expression in cholinergic, dopaminergic and vasopressinergic neurons. Eur. J. Neurosci. 18, 1593–1606.
Ben-Hur, T., Ben-Yosef, Y., Mizrachi-Kol, R., Ben-Menachem, O., Miller, A., 2006. Cytokine-mediated modulation of MMPs and TIMPs in multipotential neural precursor cells. J. Neuroimmunol. 175, 12–18.
Bovetti, S., Bovolin, P., Perroteau, I., Puche, A.C., 2007. Subventricular zone-derived neuroblast migration to the olfactory bulb is modulated by matrix remodelling. Eur. J. Neurosci. 25, 2021–2033.
Brazel, C.Y., Alaythan, A.A., Felling, R.J., Calderon, F., Levison, S.W., 2014. Molecular features of neural stem cells enable their enrichment using pharmacological inhibitors of survival-promoting kinases. J. Neurochem. 128, 376–390.
Chiba, S., et al., 2004. Anatomical and functional recovery by embryonic stem cell-derived neural tissue of a mouse model of brain damage. J. Neurol. Sci. 219, 107–117.
Cho, S.Y., et al., 2010. The effect of CXCL12 processing on CD34+ cell migration in myeloproliferative neoplasms. Cancer Res. 70, 3402–3410.
Cole, K.E., et al., 1998. Interferon-inducible T cell alpha chemoattractant (I-TAC): a novel non-ELR CXC chemokine with potent activity on activated T cells through selective high affinity binding to CXCR3. J. Exp. Med. 187, 2009–2021.
Coulson-Thomas, Y.M., et al., 2008. Adult bone marrow-derived mononuclear cells expressing chondroitinase AC transplanted into CNS injury sites promote local brain chondroitin sulphate degradation. J. Neurosci. Methods 171, 19–29.
Crump, M.P., et al., 1997. Solution structure and basis for functional activity of stromal cell-derived factor-1; dissociation of CXCR4 activation from binding and inhibition of HIV-1. EMBO J. 16, 6996–7007.
Delgado, M.B., et al., 2001. Rapid inactivation of stromal cell-derived factor-1 by cathepsin G associated with lymphocytes. Eur. J. Immunol. 31, 699–707.
Denoyer, A., et al., 2012. CXCR3 antagonism of SDF-1(5-67) restores trabecular function and prevents retinal neurodegeneration in a rat model of ocular hypertension. PLoS One 7, e37873.
Doetsch, F., Garcia-Verdugo, J.M., Alvarez-Buylla, A., 1997. Cellular composition and three-dimensional organization of the subventricular germinal zone in the adult mammalian brain. J. Neurosci. 17, 5046–5061.
Doetsch, F., Caille, I., Lim, D.A., Garcia-Verdugo, J.M., Alvarez-Buylla, A., 1999. Subventricular zone astrocytes are neural stem cells in the adult mammalian brain. Cell 97, 703–716.
Falcao, A.M., et al., 2012. The path from the choroid plexus to the subventricular zone: go with the flow! Front. Cell. Neurosci. 6, 34.
Filippo, T.R., et al., 2013. CXCL12 N-terminal end is sufficient to induce chemotaxis and proliferation of neural stem/progenitor cells. Stem Cell Res. 11, 913–925.
Hesselgesser, J., et al., 1998. Identification and characterization of the CXCR4 chemokine receptor in human T cell lines: ligand binding, biological activity, and HIV-1 infectivity. J. Immunol. 160, 877–883.
Hoehna, Y., et al., 2012. Matrix metalloproteinase 9 regulates cell death following pilocarpine-induced seizures in the developing brain. Neurobiol. Dis. 48, 339–347.
Hunt, L., et al., 2005. Low-temperature pausing of cultivated mammalian cells. Biotechnol. Bioeng. 89, 157–163.
Imitola, J., et al., 2004. Directed migration of neural stem cells to sites of CNS injury by the stromal cell-derived factor 1alpha/CXC chemokine receptor 4 pathway. Proc. Natl. Acad. Sci. U. S. A. 101, 18117–18122.
Itoh, T., et al., 2009. The relationship between SDF-1alpha/CXCR4 and neural stem cells appearing in damaged area after traumatic brain injury in rats. Neurol. Res. 31, 90–102.
Kang, S.S., et al., 2008. Inhibition of matrix metalloproteinase-9 attenuated neural progenitor cell migration after photothrombotic ischemia. Brain Res. 1228, 20–26.
Kaplan, A., et al., 2014. Neuronal matrix metalloproteinase-9 is a determinant of selective neurodegeneration. Neuron 81, 333–348.
Kokovay, E., et al., 2010. Adult SVZ lineage cells home to and leave the vascular niche via differential responses to SDF1/CXCR4 signaling. Cell Stem Cell 7, 163–173.
Lee, S.R., et al., 2006. Involvement of matrix metalloproteinase in neuroblast cell migration from the subventricular zone after stroke. J. Neurosci. 26, 3491–3495.

Levesque, J.P., Hendy, J., Takamatsu, Y., Simmons, P.J., Bendall, L.J., 2003. Disruption of the CXCR4/CXCL12 chemotactic interaction during hematopoietic stem cell mobilization induced by GCSF or cyclophosphamide. J. Clin. Invest. 111, 187–196.
Li, M., Hale, J.S., Rich, J.N., Ransohoff, R.M., Lathia, J.D., 2012. Chemokine CXCL12 in neurodegenerative diseases: an SOS signal for stem cell-based repair. Trends Neurosci. 35, 619–628.
Lim, D.A., Alvarez-Buylla, A., 2014. Adult neural stem cells stake their ground. Trends Neurosci. 37, 563–571.
Lledo, P.M., Merkle, F.T., Alvarez-Buylla, A., 2008. Origin and function of olfactory bulb interneuron diversity. Trends Neurosci. 31, 392–400.
Lois, C., Alvarez-Buylla, A., 1994. Long-distance neuronal migration in the adult mammalian brain. Science 264, 1145–1148.
Malone, C.D., et al., 2012. Mcl-1 regulates the survival of adult neural precursor cells. Mol. Cell. Neurosci. 49, 439–447.
McGrath, K.E., Koniski, A.D., Maltby, K.M., McGann, J.K., Palis, J., 1999. Embryonic expression and function of the chemokine SDF-1 and its receptor, CXCR4. Dev. Biol. 213, 442–456.
McQuibban, G.A., et al., 2001. Matrix metalloproteinase activity inactivates the CXC chemokine stromal cell-derived factor-1. J. Biol. Chem. 276, 43503–43508.
Ottoson, N.C., Pribila, J.T., Chan, A.S., Shimizu, Y., 2001. Cutting edge: T cell migration regulated by CXCR4 chemokine receptor signaling to ZAP-70 tyrosine kinase. J. Immunol. 167, 1857–1861.
Pelletier, A.J., et al., 2000. Presentation of chemokine SDF-1 alpha by fibronectin mediates directed migration of T cells. Blood 96, 2682–2690.
Peng, H., Wu, Y., Duan, Z., Ciborowski, P., Zheng, J.C., 2012. Proteolytic processing of SDF-1alpha by matrix metalloproteinase-2 impairs CXCR4 signaling and reduces neural progenitor cell migration. Protein Cell 3, 875–882.
Poznansky, M.C., et al., 2000. Active movement of T cells away from a chemokine. Nat. Med. 6, 543–548.
Ramaswamy, S., Goings, G.E., Soderstrom, K.E., Szele, F.G., Kozlowski, D.A., 2005. Cellular proliferation and migration following a controlled cortical impact in the mouse. Brain Res. 1053, 38–53.
Sacramento, C.B., Moraes, J.Z., Denapolis, P.M., Han, S.W., 2010. Gene expression promoted by the SV40 DNA targeting sequence and the hypoxia-responsive element under normoxia and hypoxia. Braz. J. Med. Biol. Res. 43, 722–727.
Saha, B., Jaber, M., Gaillard, A., 2012. Potentials of endogenous neural stem cells in cortical repair. Front. Cell. Neurosci. 6, 14.
Sonna, L.A., Fujita, J., Gaffin, S.L., Lilly, C.M., 2002. Invited review: effects of heat and cold stress on mammalian gene expression. J. Appl. Physiol. (1985) 92, 1725–1742.
Stomrud, E., Bjorkqvist, M., Janciauskiene, S., Minthon, L., Hansson, O., 2010. Alterations of matrix metalloproteinases in the healthy elderly with increased risk of prodromal Alzheimer's disease. Alzheimers Res. Ther. 2, 20.
Tham, T.N., et al., 2001. Developmental pattern of expression of the alpha chemokine stromal cell-derived factor 1 in the rat central nervous system. Eur. J. Neurosci. 13, 845–856.
Thored, P., et al., 2006. Persistent production of neurons from adult brain stem cells during recovery after stroke. Stem Cells 24, 739–747.
Tiveron, M.C., et al., 2006. Molecular interaction between projection neuron precursors and invading interneurons via stromal-derived factor 1 (CXCL12)/CXCR4 signaling in the cortical subventricular zone/intermediate zone. J. Neurosci. 26, 13273–13278.
Uckermann, O., et al., 2011. Matrix metalloproteinases 2 and 9 fail to influence drug-induced neuroapoptosis in developing rat brain. Neurotox. Res. 19, 638–648.
Uppaluri, R., et al., 2008. Prolongation of cardiac and islet allograft survival by a blocking hamster anti-mouse CXCR3 monoclonal antibody. Transplantation 86, 137–147.
Van Raemdonck, K., Van den Steen, P.E., Liekens, S., Van Damme, J., Struyf, S., 2014. CXCR3 ligands in disease and therapy. Cytokine Growth Factor Rev.
Vergote, D., et al., 2006. Proteolytic processing of SDF-1alpha reveals a change in receptor specificity mediating HIV-associated neurodegeneration. Proc. Natl. Acad. Sci. U. S. A. 103, 19182–19187.
Walton, N.M., et al., 2006. Microglia instruct subventricular zone neurogenesis. Glia 54, 815–825.
Zhang, K., et al., 2003. HIV-induced metalloproteinase processing of the chemokine stromal cell derived factor-1 causes neurodegeneration. Nat. Neurosci. 6, 1064–1071.
Zhu, Y., et al., 2009. CXCR3 activation by lentivirus infection suppresses neuronal autophagy: neuroprotective effects of antiretroviral therapy. FASEB J. 23, 2928–2941.
Zlatopolskiy, A., Laurence, J., 2001. 'Reverse gear' cellular movement mediated by chemokines. Immunol. Cell Biol. 79 (4), 340.